

Electron-spin-relaxation times in Se-doped potassium dihydrogen phosphate ferroelectric crystals

D. D. Wheeler, H. A. Farach, C. P. Poole, Jr., and R. J. Creswick

Department of Physics and Astronomy, University of South Carolina, Columbia, South Carolina 29208

(Received 10 November 1986; revised manuscript received 4 November 1987)

Electronic spin-lattice and spin-spin relaxation times, T_1 and T_2 , respectively, were measured for radiation-induced free-radical ions in selenium-doped potassium dihydrogen phosphate single crystals over the temperature range from 4.2 to 190 K. The relaxation times were determined via continuous-wave saturation and the method of Zhidkov *et al.* was used to analyze the inhomogeneously broadened spectra. In the neighborhood of the ferroelectric phase transition temperature $T_c = 123$ K, T_1 increased and T_2 decreased from their values far removed from T_c . When the data points near the phase transition were excluded, the log-log plots of $1/T_1$ versus the absolute temperature (T) exhibited a linear low-temperature region in which $1/T_1$ arises from the direct process and is proportional to T and a higher-temperature Raman-process region. The coefficients for the direct and Raman-process relaxation equations were determined, and the Debye temperature Θ was estimated to be 119 K. The behavior of T_1 near T_c can be understood in terms of a polarization cloud produced by the freezing of the local soft modes in the neighborhood of the radical ion. A mean-field treatment of this theory reproduces the cusp in T_1 at T_c .

I. INTRODUCTION

When potassium dihydrogen phosphate (KDP) undergoes a transition from the paraelectric to the ferroelectric state, the "soft modes" of vibration become dominant in the neighborhood of the phase-transition point T_c . The electron-spin-resonance spectra of radiation-induced radicals can provide information about these soft modes. Since the electronic spin-lattice and spin-spin relaxation times, T_1 and T_2 , respectively, involve interactions with the lattice vibrations, the dominance of the soft modes has a pronounced effect on the relaxation in the neighborhood of T_c . In this paper we report the details of this relaxation behavior as determined by electron-spin resonance. The system studied was KDP doped with 5 mole % K_2SeO_4 .

II. CRYSTAL STRUCTURE AND SAMPLE PREPARATION

The crystal structure of KH_2PO_4 (KDP) above 123 K consists of interpenetrating body-centered lattices of potassium atoms and PO_4 tetrahedra.¹⁻³ The phosphate tetrahedra are separated from the potassiums along the c axis of the crystal. Each of the phosphate ions is connected to four others by hydrogen bonds which are nearly perpendicular to the c axis. Above 123 K, KDP is in the paraelectric phase with space group $I\bar{4}2d$ (D_{2d}^{12}), which has four molecules of KH_2PO_4 in the unit cell. The lattice constants a and c are 7.434 Å, and 6.945 Å, respectively.

Below 123 K, the structure distorts slightly to the orthorhombic space group $Fdd2$ (C_{2v}^{19}).^{1,2} The K and P atoms move along the c axis by about 0.04 Å and 0.08 Å, respectively, when the hydrogen atoms are ordered at either near or far positions. This results in the polarization of the $K^+(H_2PO_4)^-$ groups along the c axis. The phase

transition which this crystal undergoes as $T \rightarrow T_c$ is an order-disorder type which is first order with a very small latent heat.

The evaporation method was used to prepare ~ 1 -mm³ single crystals of KDP: K_2SeO_4 by starting with a supersaturated solution slightly above room temperature. Fifteen grams of KDP and 1.326 g of K_2SeO_4 provided the 5 mole % doped crystals of KDP: K_2SeO_4 . A drop of phosphoric acid was added to aid crystal growth.⁴ The best results were found when the pyramid-shaped portion of the crystal, which is along the c axis, was placed so that the crystal was just below the surface of the liquid.

III. INSTRUMENTATION

The continuous-wave saturation ESR spectra were obtained using a Varian E Line X-band spectrometer operating in the absorption mode with a modulation frequency of 100 kHz and an amplitude of 1 G.

The pulse saturation measurements were made using a locally constructed superheterodyne X-band spectrometer. Microwave switches were employed to permit the saturation of the sample with a high-power microwave pulse and the subsequent monitoring of the recovery at low microwave powers. Various pulse lengths and duty cycles were available. The Tracor Northern digital signal analyzer was used to scan the magnetic field and to record and average the pulses and recoveries.

In this experiment, the measurement of the magnetic component H_1 of the microwave field was carried out by the method of Kooser, Volland, and Freed.⁵ A small metal sphere of radius r was placed adjacent to the sample crystal. The metal ball perturbs the magnetic field of the standing microwaves and shifts the resonant frequency f of the microwave cavity slightly from its initial value of f_0 . The value for H_1 is given by

$$H_1^2 = \frac{QP}{4\pi f_0} \frac{(f^2 - f_0^2)}{f_0^2} \frac{1}{2\pi r^3}, \quad (1)$$

where P is the incident power in watts and Q is the cavity quality factor that remains almost constant in the range of temperatures used. The experimental values used were

$$\begin{aligned} f_0 &= 9010.0 \text{ MHz}, \quad f = 9015.3 \text{ MHz}, \\ Q &= 5400, \quad r = 0.7 \text{ mm}, \end{aligned} \quad (2)$$

which gives for H_1 (G),

$$H_1 = 0.721\sqrt{P}. \quad (3)$$

IV. FREE RADICALS IN POTASSIUM DIHYDROGEN PHOSPHATE

The relaxation behavior near the transition point was studied using radiation-induced free-radical ions. Various radical ions were used in our previous work,⁶⁻¹⁰ and the present investigation was carried out with selenium-doped KDP.

The use of $K_2\text{SeO}_4$ as a dopant in KDP was first reported by Hukuda, Hanafusa, and Kawano in 1974.¹¹ The ion SeO_4^{2-} does not have an unpaired electron, and therefore does not exhibit any ESR spectra. Upon irradiation, however, the reaction



produces the SeO_4^{3-} radical ion, which is stable at room temperature, comparable in size to the PO_4^{3-} which it replaces, and has the same charge, thereby minimizing local lattice distortions.

In the paraelectric phase it is known that there are three centers,^{11,12}

$$\begin{aligned} \text{center } A \text{ (SeO}_4^{3-}), \quad I &= \frac{1}{2} \\ \text{center } B \text{ (SeO}_4^-), \quad I &= \frac{1}{2} \\ \text{center } C \text{ (superposition of SeO}_4^{3-} \text{ and SeO}_4^-), \\ I &= 0. \end{aligned} \quad (5)$$

In Fig. 1 we show the spectrum above the transition temperature with these three centers present; the strong center, line C, which is the one studied in this work, is

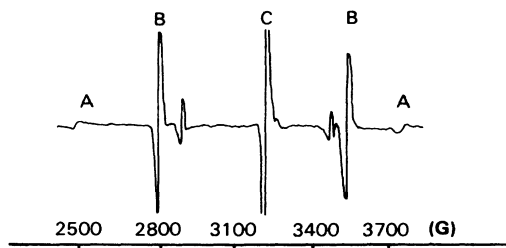


FIG. 1. ESR first-derivative absorption spectrum of x -irradiated Se-doped KDP showing the A, B, and C lines discussed in the text. The strong center, line C, is offscale.

over 100 times as intense as the other spectral lines and is shown offscale on the figure. Below the transition temperature for certain magnetic field orientations the lines split in two. Our cw radiation data show that the line is inhomogeneously broadened with increasing power levels producing considerably more change in the amplitude of the line than in the width. Therefore in interpreting these data we have made the plausible assumption¹³⁻¹⁶ that the line shape arises from a convolution of Lorentzians and Gaussians.

V. DETERMINING THE RELAXATION TIMES

The method of Zhidkov *et al.*¹⁷ was employed to determine the spin-lattice and spin-spin relaxation times, T_1 and T_2 , respectively, from the inhomogeneously broadened absorption first-derivative spectra that were obtained from the irradiated KDP. The imaginary part of the magnetic susceptibility χ'' of this line shape arises from a Gaussian distribution of width $\Delta\omega_G = \gamma\Delta H_G$ of Lorentzian-shaped spin packets of width $\Delta\omega_P = \gamma\Delta H_P$,

$$\chi'' = (1+s^2)^{1/2} \int_{-\infty}^{\infty} \frac{\left[\frac{1+s^2}{y^2} \right] \exp(-\xi^2) d\xi}{\left[\frac{1+s^2}{y^2} \right] + (x-\xi)^2}, \quad (6)$$

where

$$\begin{aligned} s^2 &= \gamma^2 H_1^2 T_1 T_2, \\ y &= \sqrt{2} \Delta\omega_P T_2, \\ x &= \frac{\omega - \omega_0}{\sqrt{2} \Delta\omega_G}. \end{aligned} \quad (7)$$

Dalal *et al.*¹² list the ratio of the p character to the s character of the unpaired electron in SeO_4^{3-} ions as $|\psi_p|^2/|\psi_s|^2 \sim 2$, which means that the unpaired electron is predominantly in the p state. The closeness of the g factor to 2 indicates that the p state is strongly quenched, as is the case for almost all free radicals. Nevertheless, the p -state character can still dominate the relaxation mechanisms. The experimental results are characterized by the peak-to-peak linewidth ΔH_{expt} of the spectrum and the microwave magnetic field values H^- and H^+ of the lower- and upper-half amplitude points, respectively, of the saturation curve shown in Fig. 2. The ratio H^+/H^- was obtained from the corresponding ratio of measured powers

$$H_1^+ / H_1^- = (P_+ / P_-)^{1/2}. \quad (8)$$

The spin-spin relaxation time is the reciprocal of the spin-packet linewidth

$$T_2 = \frac{1}{\gamma \Delta H_P}. \quad (9)$$

Zhidkov *et al.*¹⁷ showed that for the condition

$$1 \leq \frac{\Delta H_G}{\Delta H_P} \leq 100, \quad (10)$$

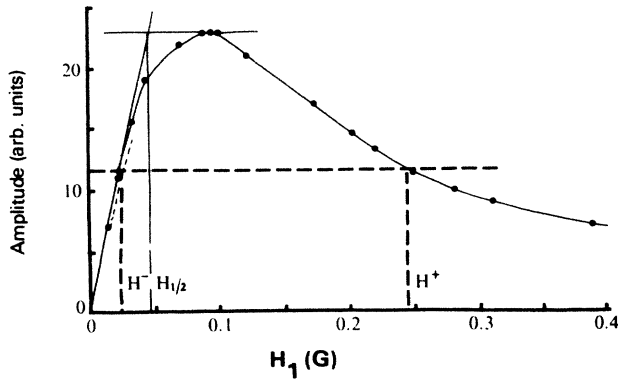


FIG. 2. Saturation curve of a partially inhomogeneously broadened C-type hyperfine line showing the construction used to determine the values of H^- , $H_{1/2}$, and H^+ .

the spin-spin relaxation time is given by

$$T_2 = \frac{(H^+/H^-) - 9}{\gamma \Delta H_{\text{expt}}} \left[\frac{\Delta H_{\text{expt}}}{\Delta H_G} \right] \quad (11)$$

$$= \left[\frac{1.14}{g} \right] \frac{(H^+/H^-) - 9}{\Delta H_{\text{expt}}} \left[\frac{\Delta H_{\text{expt}}}{\Delta H_G} \right] \times 10^{-7}, \quad (12)$$

where for the present case we use $g=2.00$. The dependence of the ratio $\Delta H_{\text{expt}}/\Delta H_G$ on the experimentally determined ratio H^+/H^- was evaluated graphically,¹⁷ with the aid of Fig. 3.

To determine the spin-lattice relaxation time T_1 , the

method of Bullock and Sutcliffe¹⁸ was employed, in which the microwave magnetic field $H_{1/2}$ is determined by finding the intersection of the low-power linear portion of the saturation curve and the horizontal tangent to the maximum point on this curve, as indicated in Fig. 2. The parameter $H_{1/2}$ is related to the value of H_1 which makes the saturation factor $s=1$ in Eq. (7), and we can write

$$T_1 = \frac{1}{T_2 \gamma^2 H_{1/2}^2 f^2}, \quad (13)$$

where f^2 is a correction factor which depends on the ratio H^+/H^- in the manner given in Fig. 4. This figure was reconstructed from Fig. 3 of the paper by Bullock and Sutcliffe.¹⁸

VI. EXPERIMENTAL RESULTS

ESR measurements were made for incident powers from 0 to 200 mW and temperatures in the range from 8 to 190 K. The crystal was oriented so that the magnetic field supplied by the magnet was perpendicular to the c axis and at 45° from the a axis of the crystal. This produced the first-derivative spectrum above the transition temperature shown in Fig. 1. The center peak, which Dalal *et al.*¹² showed was due primarily to SeO_4^{3-} , was the signal which was studied in this work.

A saturation curve of the spectral amplitude versus the H_1 field was drawn for each temperature, and the points H^- , $H_{1/2}$, and H^+ were determined from each such curve. Then the ratio H^+/H^- was calculated and the two correction factors $\Delta H_{\text{expt}}/\Delta H_G$ and f^2 were evalu-

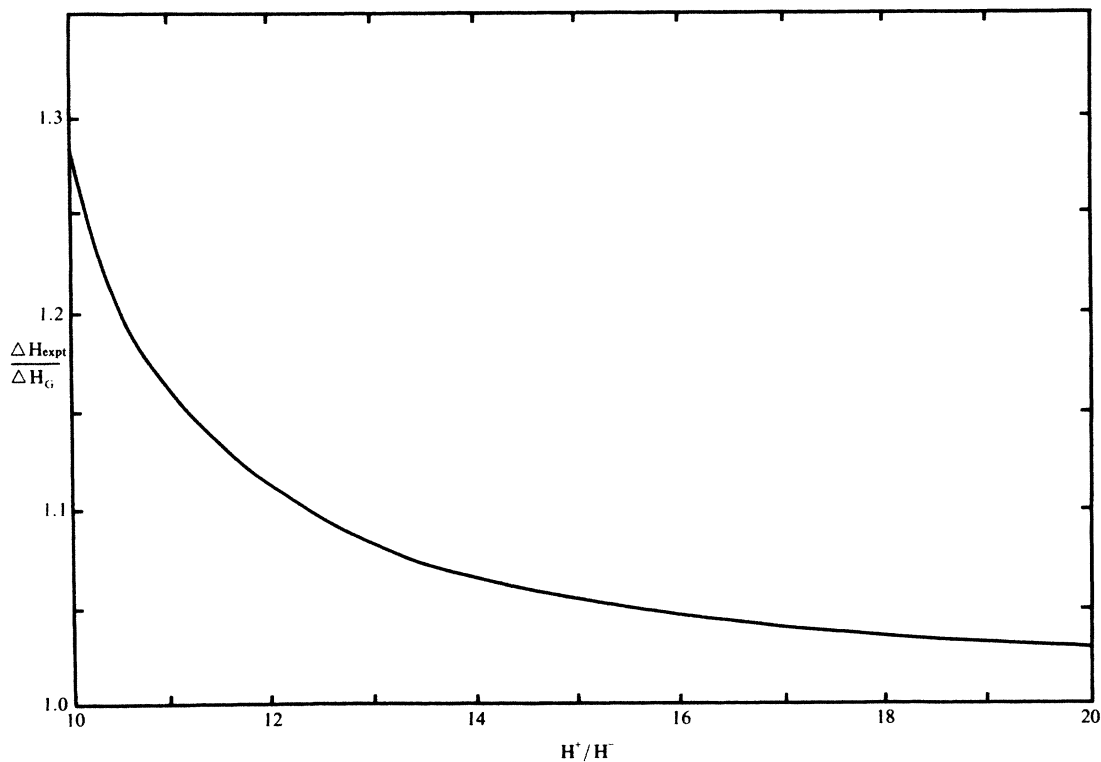


FIG. 3. Dependence of the ratio $\Delta H_{\text{expt}}/\Delta H_G$ on H^+/H^- . This graph is used in conjunction with Eq. (12) to determine T_2 .

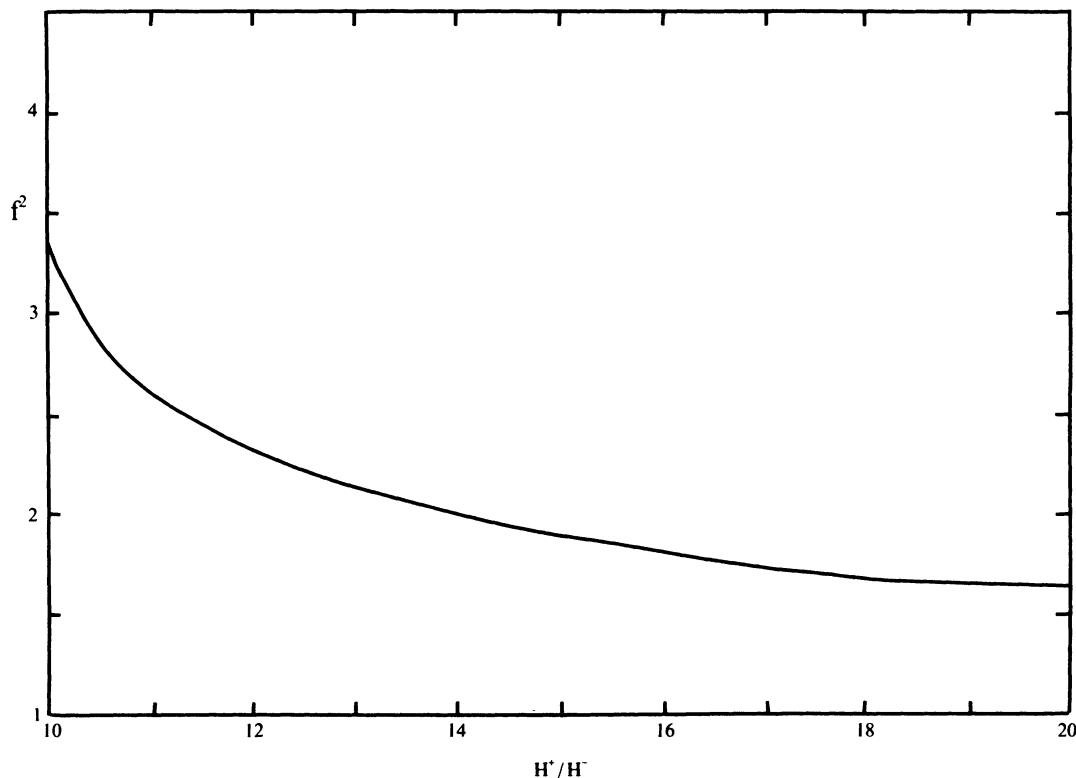


FIG. 4. Dependence of the correction factor f^2 on the ratio H^+/H^- . This graph is used in conjunction with Eq. (13) to determine T_1 .

ated from Figs. 3 and 4, respectively. These factors together with the peak-to-peak linewidth ΔH_{expt} of the spectrum at low power and the g factor $g=2.00$ were inserted into Eqs. (12) and (13) to give the values of T_2 and T_1 , respectively. Plots of the experimental points of $1/T_1$ and $1/T_2$ versus the temperature are given in Figs. 5 and 6, respectively.

VII. RELAXATION MECHANISMS

The selenate radical-ion orbital has a very-strong p character¹² and this provides a mechanism for relaxation through the van Vleck spin-orbit coupling mechanism.^{19,20}

The experimental relaxation time data were fitted to the expression²¹

$$1/T_1 = AT + BI_8(\Theta/T), \quad (14)$$

where the first term arises from the direct process, the second term is due to the Raman process, Θ is the Debye temperature, and I_8 designates the following integral:^{19,21}

$$I_8(\Theta/T) = \int_0^{k\Theta/h} \frac{\nu^8 e^{h\nu/kT} d\nu}{(e^{h\nu/kT} - 1)^2}. \quad (15)$$

Setting

$$x = h\nu/kT \quad (16)$$

we obtain

$$I_8(\Theta/T) = \left(\frac{h}{k} T \right)^9 \int_0^{\Theta/T} \frac{x^8 e^x}{(e^x - 1)^2} dx. \quad (17)$$

The linear part AT of Eq. (14) was fitted to the three lowest temperature points because the term I_8 is much smaller than AT for $T=8, 10,$ and 12 K. The fitting gave $A=102 \text{ K}^{-1} \text{ s}^{-1}$. The remaining experimental points (excluding temperatures around T_c) were fitted to the expression^{22,23}

$$1/T_1 = 102T + BI_8(\Theta/T). \quad (18)$$

To accomplish this a grid of Θ 's was calculated from Eq. (18) for various values of B and Θ with T from 28 to 190 K. Figure 7 shows the best fitting between the experimental $1/T_1$ data and the values of $1/T_1$ calculated from Eq. (18). This was obtained for $\Theta=119 \pm 5$ K and $B=4.7 \times 10^{-13} \text{ s}^{-8}$.

VIII. PULSE SATURATION

All of the relaxation times discussed to this point were measured by continuous-wave saturation. To check these results the pulse technique was employed to provide an independent value of T_1 at 4.2 K. The spin system was saturated by a pulse of about 10 ms, which was broad enough to avoid the effects of cross relaxation, and the recovery of the signal was monitored following the cessation of the pulse. The signal recovery exhibited a spin-

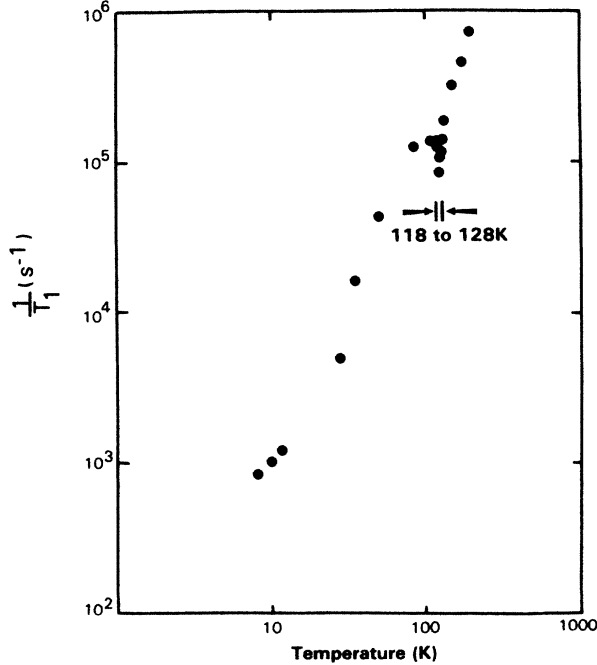


FIG. 5. Log-log plot of the dependence of the reciprocal of the measured spin-lattice relaxation time $1/T_1$ on the absolute temperature T . Note the drop in the value of $1/T_1$ in the neighborhood of the transition temperature $T_c = 123$ K.

lattice relaxation time $T_1 = 0.0029$ s at 4.2 K. This is close to the value of $T_1 = 0.0023$ s calculated from Eq. (18) for the same temperature.

IX. THEORETICAL CONSIDERATIONS

The anomalous behavior of the spin-lattice relaxation time near T_c can be understood within the pseudofreez-

ing model of Blinc and co-workers.²⁴⁻²⁶ In this theory the system is represented by an Ising model in which the coupling of the paramagnetic (PM) SeO_4^{3-} radical ion to its neighbors J' is stronger than the couplings between host atoms J . A "polarization cloud" produced by the freezing out of the local soft mode surrounds the paramagnetic ion, and in order to flip the spin at the paramagnetic site it is necessary to flip the entire polarization cloud. The relaxation time is given by a modified Arrhenius law

$$T_1(T) = \tilde{T}_1 e^{\beta V_{\text{eff}}} \quad (19)$$

$$= \tilde{T}_1 e^{\beta(F_0 - F)}, \quad (20)$$

where $V_{\text{eff}} = F_0 - F$, F_0 is the free energy in the absence of the PM ion, F is the free energy with the PM ion present, and $\tilde{T}_1(T)$ is the relaxation time in the absence of the impurity. V_{eff} represents a kind of self-induced free energy barrier which the paramagnetic ion must overcome in order to reverse its state of polarization.

The mean-field equations for the Ising model are

$$\phi(i) = \sum_j K(i, j) \tanh \phi(j), \quad (21)$$

where $\tanh \phi(i) = \langle S(i) \rangle$, $K(i, j) = \beta J(i, j)$, and $J(i, j)$ is the matrix of coupling constants. For $T > T_c$, $\phi(i)$ is small for sites far from the PM site as compared to the correlation length ξ , and we can write

$$\sum_j [\delta(i, j) - K_0(i, j)] \phi(j) = \sum_j K_1(i, j) \tanh \phi(j), \quad (22)$$

where we have separated out the matrix of extra couplings of the PM site, $K_1(i, j)$, from the host coupling matrix $K_0(i, j)$:

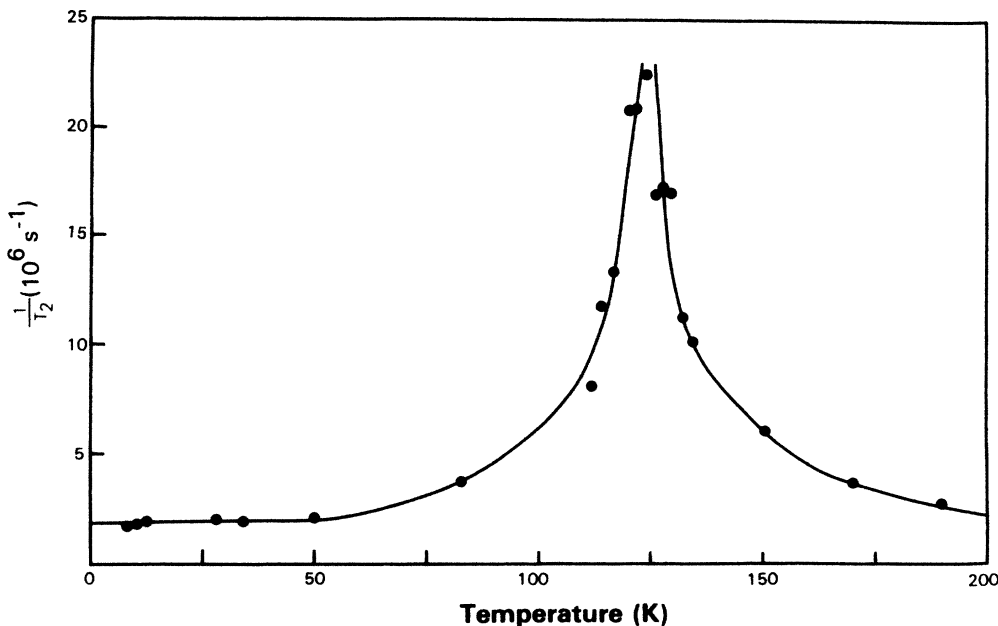


FIG. 6. Plot of the dependence of the reciprocal of the spin-spin relaxation time $1/T_2$ (points) on the absolute temperature T . The solid curve is a guide to the eye. Note the sharp rise in the value of $1/T_2$ in the neighborhood of the transition temperature $T_c = 123$ K.

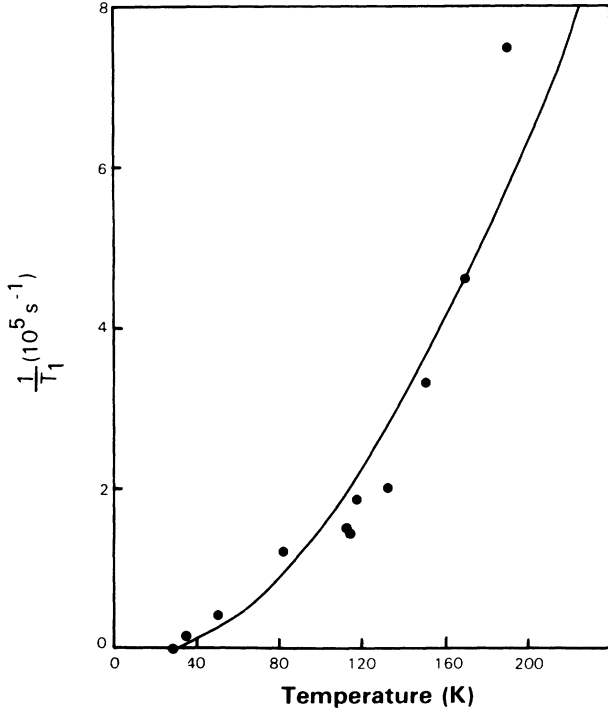


FIG. 7. Comparison of the experimentally measured spin lattice relaxation times (points) with the values (solid curve) calculated from Eq. (17) with $\Theta=119$ K and $B=4.7 \times 10^{-13}$ s $^{-8}$. The data points in the neighborhood of the transition temperature are not shown.

$$K_1(i,j) = \begin{cases} K' - K, & \text{if } i=0 \text{ and } j \text{ is NN of } 0 \\ K' - K, & \text{if } j=0 \text{ and } i \text{ is NN of } 0 \\ 0, & \text{otherwise,} \end{cases} \quad (23)$$

$$K_0(i,j) = \begin{cases} K, & \text{if } i,j \text{ are NN} \\ 0, & \text{otherwise} \end{cases} \quad (24)$$

(NN are nearest neighbors). The inverse of the operator appearing on the left-hand side of (22) is just the spin-spin correlation function (in the mean-field approximation) $G(i,j)$. Therefore we may write

$$\phi(i) = \sum_k \sum_j G(i,j) K_1(j,k) \tanh \phi(k), \quad \frac{|\mathbf{r}|}{\xi} \gg 1. \quad (25)$$

Assuming nearest-neighbor couplings only, and taking the polarization around the PM site to be saturated [$\tanh \phi(k) = 1$], this gives

$$\phi(i) \cong q(K' - K)G(\mathbf{r}_i, 0), \quad |\mathbf{r}_i| \gg \xi \quad (26)$$

where q is the number of nearest neighbors. The free energy of a solution of the mean-field equations is

$$\beta F = \frac{1}{2} \sum_i [\frac{1}{2} \phi(i) \tanh \phi(i) - \ln \cosh \phi(i)], \quad (27)$$

which for small $\phi(i)$ has the limiting form

$$\beta F \sim -\frac{1}{12} \sum_i \phi^4(i), \quad \phi(i) \ll 1. \quad (28)$$

The correlation function has the asymptotic behavior in the mean-field approximation

$$G(\mathbf{r}) \sim \frac{e^{-|\mathbf{r}|/\xi}}{|\mathbf{r}|}, \quad |\mathbf{r}| \gg \xi. \quad (29)$$

Substituting the asymptotic form of G into (26) and (27) and converting the sum over sites in (27) to an integral, the contribution of distant spins to the free energy is

$$\beta F_S = -\frac{q^4(K' - K)^4}{12} \int_{r_0}^{\infty} dr \frac{e^{-4r/\xi}}{r^2}, \quad (30)$$

where r_0 is an arbitrary distance beyond which ϕ can be considered small. Making the change of variable $r = x\xi$, (30) becomes

$$\beta F_S = -\frac{q^4(K' - K)^4}{12} \frac{1}{\xi} \int_{r_0/\xi}^{\infty} dx \frac{e^{-4x}}{x^2}. \quad (31)$$

The anomalous behavior in T_1 near T_c arises from the critical growth of the polarization cloud as $T \rightarrow T_c$. The size of the cloud is, by (26) and (29), given by the correlation length ξ , which in mean-field theory diverges as

$$\xi \sim \left[\frac{T - T_c}{T_c} \right]^{-1/2}. \quad (32)$$

In the limit $\xi \rightarrow \infty$, (31) becomes

$$\beta F_S = -\frac{q^4(K' - K)^4}{12} \left[\frac{1}{r_0} - \frac{4}{\xi} + \dots \right]. \quad (33)$$

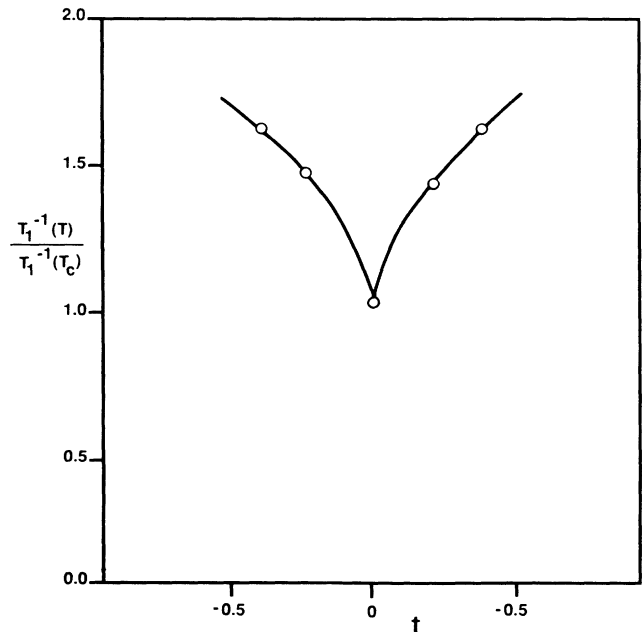


FIG. 8. Comparison of the experimentally measured spin-lattice relaxation times in the neighborhood of the transition temperature with the values calculated from Eq. (36).

In addition to this "singular" contribution to the free energy there is also a contribution from the nearby spins, $r_i < r_0$, which, together with the first term in (33), is relatively insensitive to temperature near T_c . Using Eqs. (32) and (33), Eq. (20) may now be cast in the form

$$\frac{1}{T_1} = \frac{1}{T_1(T_c)} e^{Bt^{1/2}}, \quad (34)$$

where $t = |T - T_c| / T_c$ and B is a constant independent of the temperature. For a simple cubic lattice

$$B = \frac{9\sqrt{6}}{8\pi^3} \left[\frac{J' - J}{J} \right]^4. \quad (35)$$

In the neighborhood $t \ll 1$ of the phase transition temperature the exponential of Eq. (34) can be expanded to give the following temperature dependence:

$$\frac{1}{T_1} = \frac{1}{T_1} (T_c)^{(1+Bt^{1/2})}, \quad (36)$$

where $T_1^{-1}(T_c) = 0.90 \times 10^5 \text{ s}^{-1}$ is the value of T_1^{-1} at T_c and the coefficient $B = 2.43$. Figure 8 shows the fitting.

X. CONCLUSIONS

In this paper we have measured the electronic spin-lattice T_1 and spin-spin T_2 relaxation times of radiation-induced free radical ions in potassium dihydrogen phosphate. We found that in the neighborhood of the phase transition temperature $T_c = 123 \text{ K}$, the value of T_1 increased and T_2 decreased from their values far removed from T_c . A mean-field treatment based on the Ising model reproduced the cusp of T_1 at T_c .

ACKNOWLEDGMENT

This work was supported by U.S. National Science Foundation Grant No. DMR-850 6690.

- ¹B. C. Frazer and R. Pepinski, *Acta Crystallogr.* **6**, 273 (1953).
²G. E. Bacon and R. S. Pease, *Proc. R. Soc. London, Ser. A* **230**, 359 (1955).
³R. J. Nelures, *Ferroelectrics* **24**, 237 (1980).
⁴A. Holden and P. Singer, *Crystals and Crystal Growing* (Anchor, New York, 1960), pp. 93–105.
⁵R. G. Kooser, W. V. Volland, and J. H. Freed, *J. Chem. Phys.* **50**, 5243 (1969).
⁶R. D. Truesdale, H. A. Farach, and C. P. Poole, Jr., *Phys. Rev. B* **22**, 365 (1980).
⁷R. D. Truesdale, C. P. Poole, Jr., and H. A. Farach, *Phys. Rev. B* **25**, 474 (1982).
⁸R. D. Truesdale, C. P. Poole, Jr., and H. A. Farach, *Phys. Rev. B* **27**, 4052 (1983).
⁹R. D. Truesdale, H. A. Farach, and C. P. Poole, Jr., *Phys. Rev. B* **28**, 5268 (1983).
¹⁰D. D. Wheeler, H. A. Farach, and C. P. Poole, Jr., *Phys. Lett.* **103A**, 144 (1984).
¹¹K. Hukuda, H. Hanafusa, and T. Kawano, *J. Phys. Soc. Jpn.* **36**, 1043 (1974).
¹²N. S. Dalal, J. A. Hebden, D. E. Kennedy, and C. A. McDowell, *J. Chem. Phys.* **66**, 4425 (1977).
¹³H. A. Farach and H. Teitelbaum, *Can. J. Phys.* **45**, 2913 (1967).
¹⁴C. P. Poole, Jr. and H. A. Farach, *Relaxation in Magnetic*

- Resonance* (Academic Press, New York, 1971), Sec. S.2.
¹⁵C. P. Poole, Jr., *Electron Spin Resonance* (Wiley, New York, 1953), Sec. 12G.
¹⁶T. G. Castner, *Phys. Rev.* **115**, 1506 (1959).
¹⁷O. P. Zhidkov, V. I. Murotsev, I. G. Akhvedianai, S. N. Safronove, and V. V. Kopylov, *Fiz. Tverd. Tela (Leningrad)* **9**, 1403 (1967) [*Sov. Phys.—Solid State* **9**, 1095 (1967)].
¹⁸A. T. Bullock and L. H. Sutcliffe, *Trans. Faraday Soc.* **60**, 2112 (1964).
¹⁹G. E. Pake, *Paramagnetic Resonance* (Benjamin, New York, 1962), Chap. 6.
²⁰V. Weisensee, G. Völkel, and W. Brunner, *Solid State Commun.* **48**, 309 (1983).
²¹W. Brunner, G. Völkel, W. Windsch, I. N. Kurkin, and V. I. Shlenkin, *Solid State Commun.* **26**, 853 (1978).
²²W. Windsch and G. Völkel, *Ferroelectrics* **24**, 195 (1980).
²³S. A. Al'tshuler and B. M. Kozyrev, *Electron Paramagnetic Resonance* (Academic, New York, 1964).
²⁴R. Blinc and P. Prelovsek, *Solid State Commun.* **42**, 893 (1984).
²⁵N. S. Dalal, R. Blinc, P. Prelovsek, and A. H. Reddoch, *Solid State Commun.* **43**, 887 (1982).
²⁶G. M. Ribeiro, L. V. Gonzaga, A. S. Chaves, R. Gazzinelli, R. Blinck, P. Ceve, P. Prelovsek, and N. I. Silkin, *Phys. Rev. B* **25**, 311 (1982).